

Double diffusion encoded MRI to identify Alzheimer's disease pathology in postmortem brainstem by Diffusion Tensor Subspace Imaging (DiTSI)

Courtney J Comrie¹, Victor Sandrin¹, Laurel Dieckhaus¹, Geidy Serrano², Thomas G Beach², Mark Bondi³, Seraphina Solders⁴, Vitaly Galinsky⁴, Lawrence R Frank⁴, and Elizabeth Hutchinson¹

¹Biomedical Engineering, University of Arizona, Tucson, AZ, United States, ²Banner Sun Health Research Institute, Sun City, AZ, United States, ³Department of Psychiatry, University of California San Diego, La Jolla, CA, United States, ⁴University of California San Diego, La Jolla, CA, United States

Synopsis

Keywords: Microstructure, Diffusion Acquisition, Double Diffusion Encoding

Motivation: Diffusion MRI may provide clinically relevant markers of degenerative pathology in Alzheimer's disease if the specificity of the frameworks can be improved. Double diffusion encoding frameworks are promising for their improved selectivity.

Goal(s): Optimization of methods and initial description of alterations in postmortem brainstem imaging with diffusion MRI including single diffusion frameworks of DTI and MAP-MRI as well as the DDE DiTSI framework.

Approach: High-resolution, high-quality diffusion MRI scans over a comprehensive encoding range were used to map metric in healthy and AD pathologic brain stem tissue

Results: Four anisotropy metrics across the three frameworks were different in contrast and alteration with pathology.

Impact: If double diffusion encoding MRI can be optimized for the detection of specific pathology in Alzheimer's disease and other brain disorders, a new class of improved imaging markers may be possible.

Introduction

It is widely hypothesized that the brain stem is affected early during the course of Alzheimer's disease (AD) although MRI markers in this region are scarce. Diffusion MRI (dMRI), can potentially capture cellular changes that accompany or precede neurodegeneration and we have recently reported that microscale anisotropy changes can be detected in the temporal lobe at earlier stages of AD than other MRI alterations¹ using the mean apparent propagator^{2,3}. However, single diffusion encoding (SDE) frameworks are known to have fundamental limitations from their sensitivity to all water displacement within the voxel. Double diffusion encoding (DDE) frameworks can overcome this limitation, but their implementation in the brain is challenging. Recently, the diffusion tensor subspace imaging (DiTSI) framework⁴ was developed which relates the DDE signal and the spin density function ϕ describing water displacement. Two new metrics for microstructure are generated from DiTSI - spherical anisotropy (SA) which is driven by angular variance of ϕ and radial anisotropy (RA) which is driven by the radial variance of ϕ . In the context of AD brain stem pathology, we expect that these metrics may provide complementary information when compared to SDE metrics such as fractional anisotropy (FA) of DTI and propagator anisotropy (PA) of MAP-MRI. The objective of the present study was to evaluate differences across DTI, MAP-MRI and DiTSI metrics for the detection of AD related brain stem pathology.

Methods

High-quality brain stem specimens (Figure 1) were obtained from the Banner Sun Health Brain and Body Donation Program⁵. The healthy control (HC) included both hemispheres and the entire pons and medulla and was taken from a patient at autopsy with no diagnosis of dementia during life. The AD specimen was a smaller tissue block from a single hemisphere from a brain with confirmed Braak score⁶ of VI and maximum plaque and tangle scores (3) in temporal lobe and pons. For both specimens, the tissues were immersed in fixative immediately following autopsy for 48 hours and then moved to phosphate buffered saline with Na-Azide (0.01%) for rehydration and storage. The samples were prepared in custom holders for MRI and immersed in Fluorinert. Specimens were imaged using a Bruker 7T MRI scanner and quadrature RF coils (86mm for HC and 40mm for AD specimens). We used Paravision 360 v3.5 to collect high resolution anatomical (HRA) images with a FLASH pulse sequence and 100 micron isotropic resolution. A T1-weighted selective inversion recovery pulse sequence with TE/TR/IR=8.5/1565/575ms was optimized for contrast of the locus coeruleus and used to visualize that structure in the HC brain stem (Figure 2). The LC was not found in the AD specimen. Diffusion MRI was collected using a 3D EPI pulse sequence. For SDE acquisition (Figure 3), the resolution was 300 microns isotropic with TE/TR=41/800ms, segments=4 and multi-shell encoding with $b(\text{ndirs})=250(6), 500(6), 1000(6), 1500(32), 3000(32), 4500(56), 6000(56)$. For DDE acquisition, the resolution was 500 microns isotropic, TE/TR=64/800ms, segments=6 and for both blocks $\delta=5\text{ms}, \Delta=20\text{ms}$ and $\tau_m=8.5\text{ms}$. The DiTSI framework requires "subspace" sampling in which the direction sets of the first and second encoding blocks are identical, but the range and combination of gradient strengths are flexible. We used cubic encoding (Figure 4) which has 64 DWIs and we repeated this for 6 different b-value combinations: $b_1/b_2=1000/1000, 1000/2000, 1000/4000, 2000/2000, 2000/4000$ and $4000/4000$ s/mm². We collected 6 unweighted images for a total of 390 DWIs in the DDE acquisition for each specimen. RA and SA maps were generated using the DiTSI framework by custom software. Histogram analysis was performed in R software (v4.2.2) using similar region of interest masks in both specimens include all regions of the AD partial sample.

Results and Discussion

High-resolution and high image quality maps were generated for the DTI, MAP and DiTSI metrics and all metrics showed prominent differences between HC and AD tissue. PA was the only metric to show a diffuse reduction in the AD specimen while FA, SA and RA showed regions of increased values with complementary and distinct spatial organization across metrics. These findings are in contrast to our observations in temporal lobe tissue and are potentially related to preferential loss of gray matter microstructure and increased volume fraction of remaining white matter, which is predominant in the brainstem. Likely multiple other pathologic alterations are concurrent and the correspondence between these and extension to additional specimens are the subject of ongoing work in this project.

Conclusions

Initial prominent findings in AD brain stem tissue suggest that metric differences across SDE and DDE frameworks can measure different and selective microstructural features of pathology in the human brain.

Acknowledgements

This research was supported by NIA/NIH grants R03AG071903 and R01AG079280. All MR imaging was performed in the UA translational biomedicine resource (TBIR) and made possible by the NIH small instrumentation grant: S10 OD025016. All image processing was performed using the UA High Performance Computing (HPC) resources. The Brain and Body Donation Program has been supported by the National Institute of Neurological Disorders and Stroke (U24 NS072026 National Brain and Tissue Resource for Parkinson's Disease and Related Disorders), the National Institute on Aging (P30 AG19610 and P30AG072980, Arizona Alzheimer's Disease Center), the Arizona Department of Health Services (contract 211002, Arizona Alzheimer's Research Center), the Arizona Biomedical Research Commission (contracts 4001, 0011, 05-901 and 1001 to the Arizona Parkinson's Disease

Figures



Figure 1. One healthy and one pathologic brainstem specimen (left) were scanned in this study. A high resolution anatomical and diffusion MRI map for directionally encoded color are shown for the healthy specimen (right).

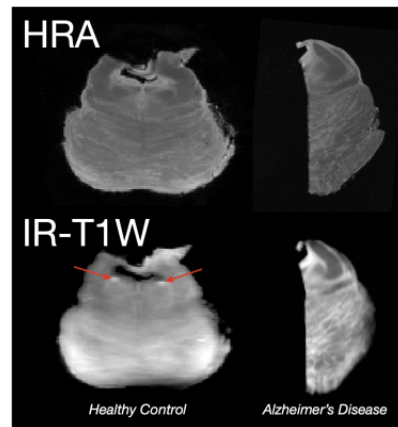


Figure 2. Inversion recovery, T1-weighted MRI (bottom row) was optimized to show locus coeruleus (LC) contrast (red arrows). Positive identification of the LC was not possible in the AD specimen (right)

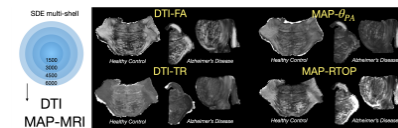


Figure 3. Single diffusion encoding (SDE) DWIs were collected over a range of b-values to support the diffusion tensor imaging (DTI) and mean apparent propagator (MAP) MRI frameworks. Metric maps are shown in both specimens for anisotropy metrics (top row) and diffusivity/restriction metrics (bottom row).

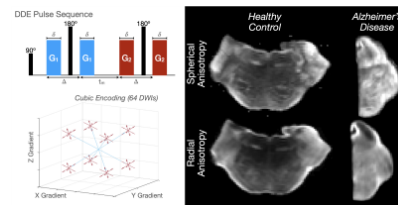


Figure 4. Double diffusion encoding (DDE) to support the Diffusion tensor subspace imaging (DiTSI) framework. 6 sets of cubic encoded data were collected with $b_1/b_2=1000/1000, 1000/2000, 1000/4000, 2000/2000, 2000/4000$ and $4000/4000$ s/mm². Spherical and Radial Anisotropy maps are shown for both specimens (right).

References

1. Comrie, C. J. et al. Identification of diffusion, kurtosis, and propagator MRI markers of Alzheimer's disease pathology in post-mortem human tissue. *Imaging Neuroscience* 2, 1-19 (2024).
2. Avram, A. V. et al. Clinical feasibility of using mean apparent propagator (MAP) MRI to characterize brain tissue microstructure. *NeuroImage* 127, 422-434 (2016).
3. Özarlan, E. et al. Mean apparent propagator (MAP) MRI: a novel diffusion imaging method for mapping tissue microstructure. *NeuroImage* 78, 16-32 (2013).
4. Frank, L. R., Zahneisen, B. & Galinsky, V. L. JEDI: Joint Estimation Diffusion Imaging of macroscopic and microscopic tissue properties. *Magn Reson Med* 84, 966-990 (2020).
5. Beach, T. G. et al. Arizona Study of Aging and Neurodegenerative Disorders and Brain and Body Donation Program. *Neuropathology* 35, 354-389 (2015).
6. Braak, H., Thal, D. R., Ghebremedhin, E. & Del Tredici, K. Stages of the pathologic process in Alzheimer disease: age categories from 1 to 100 years. *J Neuropathol Exp Neurol* 70, 960-969 (2011).

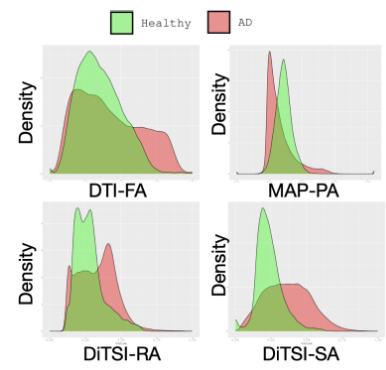


Figure 5. Histogram plots for all values in a corresponding region of interest to the smaller AD specimen for the healthy and AD metric maps.